

OPTICAL RADIATION SOURCES

PACS numbers: 42.55.Px; 78.67.–n; 42.25.Kb; 42.30.Wb
DOI: 10.1070/QE2013v043n08ABEH015124

Broadband superluminescent diodes with bell-shaped spectra emitting in the range from 800 to 900 nm

E.V. Andreeva, S.N. Il'chenko, Yu.O. Kostin, M.A. Ladugin,
P.I. Lapin, A.A. Marmalyuk, S.D. Yakubovich

Abstract. **Quantum-well superluminescent diodes (SLD) with extremely thin active (AlGa)As and (InGa)As layers and centre wavelengths about 810, 840, 860 and 880 nm are experimentally studied. Their emission spectrum possesses the shape close to Gaussian, its FWHM being 30–60 nm depending on the length of the active channel and the level of pumping. Under cw injection, the output power of light-emitting modules based on such SLDs can amount to 1.0–25 mW at the output of a single-mode fibre. It is demonstrated that the operation lifetime of these devices exceeds 30000 hours. Based on the light-emitting modules the prototypes of combined BroadLighter series light sources are implemented having a bell-shaped spectrum with the width up to 100 nm.**

Keywords: *nanoheterostructure, quantum-well superluminescent diode, optical coherence tomography.*

1. Introduction

The most important characteristic of low-coherence light sources used in time-domain and Fourier-domain optical coherence tomography (OCT) systems [1] is the autocorrelation function (ACF), or coherence function, which is defined as a Fourier transform of the radiation spectrum and can be measured, e.g., as the dependence of the interference pattern visibility on the optical path difference in a symmetric Michelson interferometer. The width of the ACF principal central maximum corresponds to the radiation coherence length $L_{\rm coh} \approx \lambda_c^2/\Delta\lambda$, where λ_c is the centre wavelength, and $\Delta\lambda$ is the optical spectrum half-width. This quantity determines the axial resolution of the obtained tomograms. The presence of additional maxima, adjacent to the principal one or remote from it, reduces the signal-to-noise ratio and worsens the quality of the obtained images. The ACF of radiation ideal for OCT must possess a solitary narrow maximum, corresponding to the zero optical path difference. Such an ACF is typical for the radiation having broad and smooth spectrum with the Gaussian shape:

$$S(\lambda) = S_0 \exp[-\gamma(\lambda - \lambda_c)^2]. \quad (1)$$

The light sources that have found the widest application in the above OCT systems are semiconductor superluminescent diodes (SLDs). The traditional SLDs with a 'bulk' active layer have the spectrum shape very close to Gaussian. Such SLDs with the centre wavelength in the range 820–840 nm have been used in the first commercial medical OCT system 'Stratos' (Carl Zeiss Meditec). These SLDs, based on the double-sided separate-confinement heterostructure (GaAl)As

E.V. Andreeva, S.N. Il'chenko, Yu.O. Kostin, P.I. Lapin Superlum Diodes Ltd., P.O. Box 70, 119454 Moscow, Russia;
M.A. Ladugin, A.A. Marmalyuk Open Joint-Stock Company 'M.F. Stelmakh Polyus Research and Development Institute', ul. Vvedenskogo 3, block 1, 117342 Moscow, Russia;
e-mail: M.Ladugin@siplus.ru, marm@siplus.ru;
S.D. Yakubovich Moscow State Institute of Radio-Engineering, Electronics and Automation (Technical University), prosp. Vernadskogo 78, 119454 Moscow, Russia;
e-mail: yakubovich@superlumdiodes.com

Received 27 December 2012; revision received 28 February 2013
Kvantovaya Elektronika **43** (8) 751–756 (2013)
Translated by V.L. Derbov

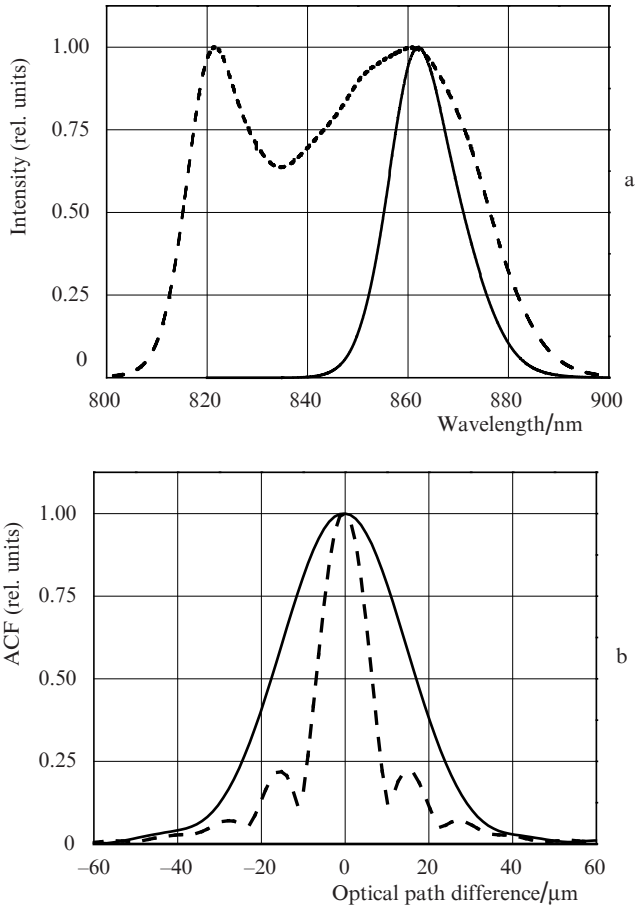

Figure 1. (a) Typical spectra and (b) ACF central peaks of the bulk (solid curves) and quantum-well (dashed curves) SLD.

with a single-mode active channel a few micrometres thick, possess the emission spectrum width of 15–20 nm, the output optical power being as large as a few tens of mW.

Later on the quantum-well SLDs operating in the same spectral range and having the active layer thickness of the order of 10 nm were designed [2–4]. Due to the contribution to superfluorescence from the quantum transitions not only from the ground, but also from the excited subband, the width of their spectrum can reach 100 nm. Such SLDs have found widest application in OCT systems, since their use allows a considerable increase in spatial resolution. However, these SLDs have a double-humped spectrum shape far from Gaussian and a pedestal under the central ACF maximum, which cannot but spoil the quality of the obtained images. Typical spectra and ACF of bulk and quantum-dimensional SLDs are presented in Fig. 1.

In quantum-well SLDs with thin (units of nanometres) active layers the excited subband is shifted towards the high-energy region. In this case at reasonable direct injection current densities (at least, in SLDs with the length L_a of the active channel being large enough) the excited subband is not filled and the superluminescence spectrum is determined by the quantum transitions from the ground subband only. The spectrum shape of such SLDs is also close to Gaussian, and the spectrum width strongly depends on the length L_a and the pump level and can exceed 60 nm. The present paper is devoted to the study of light sources based on SLDs of this type.

2. Experimental samples

The experimental samples of the SLDs were fabricated from semiconductor double-sided heterostructures with a separate confinement of the photon field and charge carriers (SC DHS) with the geometry and composition of the contact, emitter and waveguide layers standard for (AlGa)As systems. Their specific feature was the design of the quantum-well active region that provided the possibility to obtain the centre wavelength of the amplified spontaneous emission at different points of the 800–900 nm spectral region and allowed strong 'driving apart' of the spectral peaks corresponding to quantum transitions from the ground and excited states. The solution of this problem is impossible using GaAs quantum wells that are traditional for heterostructures of this spectral range. The calculations carried out have shown that the practical implementation of the above parameters requires the use of strained ultrathin quantum wells consisting of (AlGa)As or (InGa)As solid solutions with a small content of Al or In. This approach enables an increase in the quantum well potential barrier height, which, together with its small width, offers a possibility to increase the separation between the size quantisation levels up to necessary values. In the calculations we used the model of a rectangular quantum well.

The heterostructures were grown using the method of low-pressure metal-organic vapour phase epitaxy on GaAs (100) substrates in a horizontal flow-type reactor. The precursors of the Group III elements were trimethylaluminum, triethygallium, and trimethylindium; the arsenic precursor was 100% arsine; and hydrogen was used as a carrier gas. The mixture of silane with hydrogen and diethylzinc were used as n- and p-dopants, respectively. The growth temperature was varied from 640 to 770 °C and the pressure in the reactor was 60–65 Torr. In the course of the present work 12 quantum-well heterostructures were grown, differing in composition and the active layer thickness d_a, which varied within the limits 4.5–9.0 nm. From each epitaxial plate a few sets of single transverse mode SLDs were fabricated that differed in the length L_a only. The experimental studies of physical characteristics of these SLDs provided statistically reliable information about the dependence of output parameters in the samples with similar radiation wavelengths on the thickness of their active layer, as well as about the output parameters of the samples with similar thickness of the active layer and different composition.

The SLD design was traditional. The active channel had the form of a ridge waveguide about 0.25 μm thick and 4 μm wide, the channel axis being inclined at an angle of 7° with respect to the normal to the faces of the AR-coated crystal. The length L_a was varied from 700 to 1600 μm. The measurements were performed under cw injection at the temperature 25 °C.

3. Experimental results

Figure 2 shows typical light–current characteristics and dependences of the full width at half maximum (FWHM) of the radiation spectrum on the injection current in a bulk SLD and in one of the studied quantum-well SLDs. The samples had absolutely similar design and composition of heterolayers, the thickness of the active layer being d_a^{bulk} = 28 nm (GaAs) and d_a^{SQW} = 6.5 nm ($In_{0.04}Ga_{0.96}As$), respectively. Their superluminescence spectra drastically differ from each other both in width and in the character of its dependence on

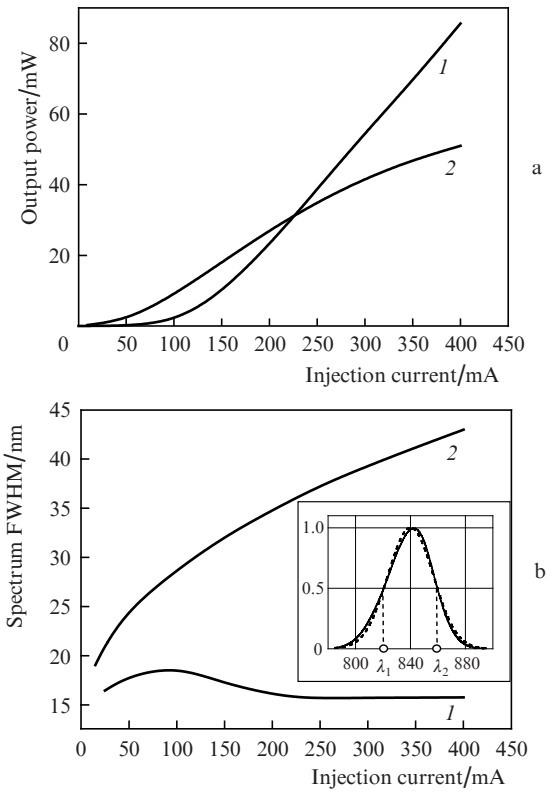

Figure 2. (a) Typical light–current characteristics and (b) dependences of the spectrum FWHM on the injection current for (*1*) the bulk and (*2*) quantum-well SLDs (d_a^{bulk} = 28 nm, d_a^{SQW} = 6.5 nm, L_a = 1200 μm, channel width W = 4 μm). The inset shows the approximation of the quantum-well SLD spectrum with a Gaussian function (dotted curve).

Table 1. Characteristics of the SLD with the $In_{0.08}Ga_{0.92}As$ active layer with the thickness $d_a^{SQW} = 4.5$ nm at the injection current density $J \approx 5.5$ kA cm^{-2}.

L_a/μm	I/mA	J/kA cm^{-2}	P_{FS}/mW	P_{SM}/mW	λ_m/nm	$\Delta\lambda$/nm	L_{coh}/μm	P_{TE}/P_{TM}
700	160	5.7	3.3	1.5	837	50	14	9.0
900	190	5.3	10.5	5.8	839	42	17	13
1100	240	5.5	24.5	15	840	36	20	19
1300	280	5.4	47	29	845	31	23	22
1600	350	5.5	77	45	850	26	28	28

Note: I is the injection current; P_{FS} is the output power in free space; P_{SM} is the output power via a single-mode optical fibre; λ_m is the median wavelength; P_{TE}/P_{TM} is the polarisation ratio.

the pump level. The spectrum shape of both samples is close to Gaussian. The inset in Fig. 2b shows the approximation of the spectrum of the quantum-well SLD by curve (*1*) at $\lambda_c = (\lambda_1 + \lambda_2)/2$ and $\gamma = (-4\ln 0.5)/(\lambda_2 - \lambda_1)^2$, which provides the equality of half-widths. The minor asymmetry of the spectral curve practically does not affect the 'purity' of the central ACF peak.

The spectral density of spontaneous radiation in the operation regimes, characteristic for SLDs, cannot be directly measured. As for the spectrum of the single-pass gain $G(\lambda) = \exp[g(\lambda) - \alpha]L_a$, where α is the dissipative loss coefficient, it can be measured with enough accuracy in the samples of semiconductor optical amplifiers (SOA) using a tunable laser operating in the appropriate spectral range as a generator of the input signal. The results of such measurements for the TE mode of SOA samples made of the same SC DHS as the SLD samples, compared above, are presented in Fig. 3. The presented curves qualitatively well agree with the behaviour of the curves in Fig. 2b. This fact shows that the width of the luminescence spectrum is determined mainly by the shape of the optical gain spectrum.

Typical output characteristics of the SLD with the active layer 4.5 nm thick at different active channel lengths and similar injection current densities are presented in Table 1. As could be expected, with the increase in L_a the radiation power and the degree of polarisation increase and the spectral width decreases.

The wavelength about 840 nm is most popular for SLD modules used in OCT systems. We have grown a set of similar-type quantum-well SC DHS with different thickness of the active layer, in which at the expense of varying the chemical composition of the solid solution (In and Ga concentration) the wavelength λ_m was kept near 840 nm. Figure 4 shows the values of the output power and the FWHM of the spectral at the typical operation injection current density for SLDs, made of these heterostructures, possessing a quasi-Gaussian shape of the spectrum and different L_a. 'Short' SLDs with 'thick' active layers at the present current density demonstrate a double-humped spectrum. The most important of the obtained results is a very weak dependence of the basic SLD parameters on the active layer thickness. This is a profitable advantage of the considered devices as compared to the SLDs with double-humped spectrum and equalised spectral maxima (series SLD-37, SLD-35 with $d_a^{SQW} \approx 10$ nm), in which

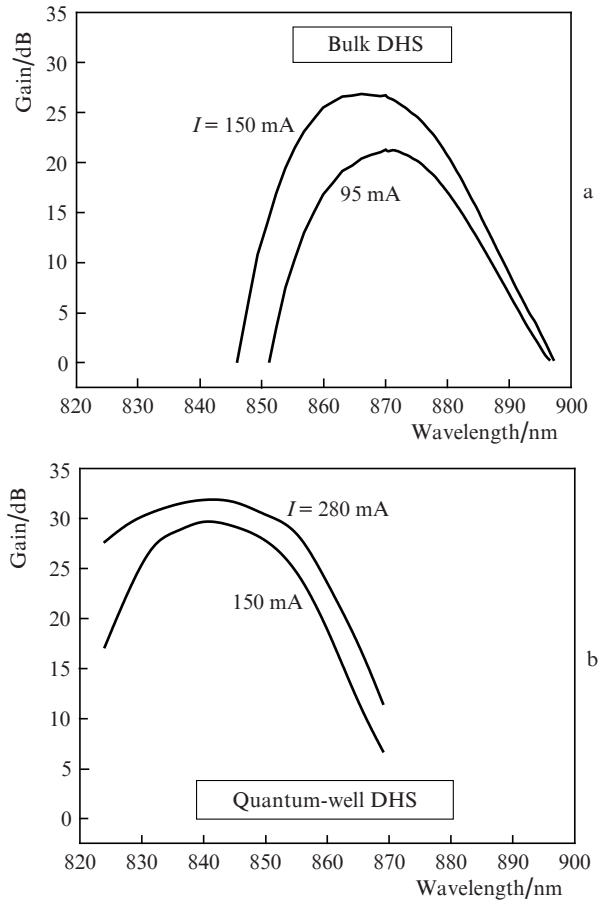

Figure 3. Small-signal gain spectra of a SOA on the basis of (a) a bulk (L_a =1200 μm) and (b) quantum-well (L_a = 1600 μm) SC DHS.

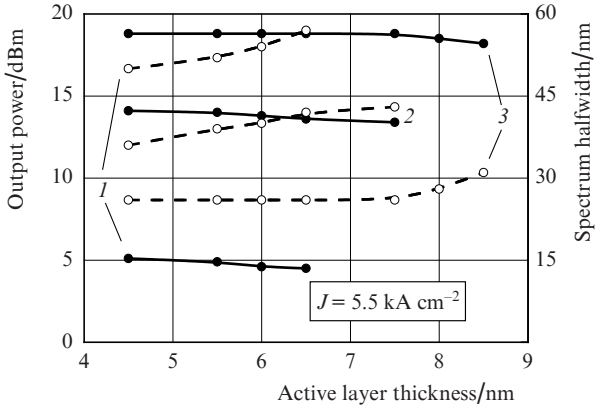

Figure 4. Output power (solid curves) and FWHM of the bell-shaped spectrum (dashed curves) vs. the thickness of the active layer for quantum-well SLDs with the median wavelength near 840 nm at L_a= (*1*) 700, (*2*) 1100 and (*3*)1600 μm.

even a slight variation of d_a^{SQW} leads to a significant change in the spectral characteristics, which hampers obtaining reproducible results in mass production. In future serial production of the considered devices it is supposed to use the value of d_a^{SQW} near 6.0 nm.

The change in the chemical composition of the SC DHS active layer, its thickness being kept constant, allows wide-range changes in the median wavelength λ_m of the manufactured SLDs. When λ_m is shifted towards the short-wavelength spectral region, the spectral width $\Delta\lambda$ is somewhat narrower, while the rest output characteristics demonstrate minor changes. Figure 5 presents typical spectra of four types of quantum-well SLDs studied by us. Table 2 summarises the basic characteristics of these SLDs at L_a = 700, 900, 1100 and 1300 μm. The chosen operation points allow obtaining the power of nearly 1.0, 3.0, 10 and 20 mW at the output of the single-mode optical fibre. Note, that the low-power 'short' SLDs possess record-breaking spectral width of about 60 nm.

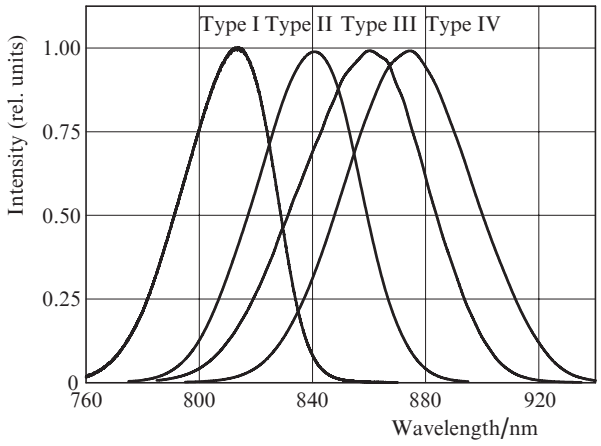

Figure 5. Typical emission spectra of the SLD with different composition of the active layer (d_a^{SQW} = 6.0 nm).

The performed life tests demonstrated sufficiently high reliability of the developed SLDs. A chronogram of one of such tests is presented in Fig. 6. The SLD spectral characteristics were measured before the beginning of the test and then each 3000 hours of continuous operation. It is important to note that after 9000 hours of operation (1 year) the deviations of λ_m and $\Delta\lambda$ values did not exceed 0.3% and 2.0%, respectively. The extrapolation of the presented curves allows estimation of the median lifetime to be 35000 hours.

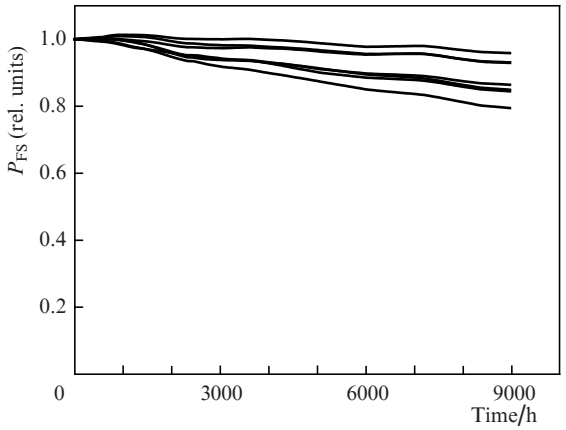

Figure 6. Chronogram of lifetest of type II SLDs (L_a = 1400 μm, $P_{FS} \approx$ 35 mW).

The performed studies allowed starting the serial production of light-emitting modules of the new SLD-34 series, including 24 models, which differ in output characteristics and housing types. Figure 7 illustrates the comparison of spectral characteristics of the new devices with those of the SLD-37 devices possessing a double-humped shape of the spectrum.

Table 2. Characteristics of I–IV type SLDs with different compositions of the active layer ($d_a^{SQW} \approx$ 6.0 nm) and active channel lengths.

Active layer composition and SLD type	L_a/μm	I/mA	J/kA cm^{-2}	P_{FS}/mW	P_{SM}/mW	λ_m/nm	$\Delta\lambda$/nm	L_{coh}/μm	P_{TE}/P_{TM}
$Al_{0.02}Ga_{0.98}As$ (type I)	700	150	5.4	2.1	0.9	806	43	15	3
	900	200	5.5	6.5	3.0	806.5	35.5	18	4
	1100	250	5.7	18	10	807.5	33	20	6
	1300	260	5.0	32	19	809	27	24	10
$In_{0.05}Ga_{0.95}As$ (type II)	700	160	5.7	3.2	1.3	835	57	12	5
	900	180	5.0	8.5	4.1	840	46	15	7
	1100	240	5.5	24	13	844	42	17	15
	1300	280	5.4	46	24	847	34	21	25
$In_{0.09}Ga_{0.91}As$ (type III)	700	170	6.1	2.5	1.2	856	58	13	6
	900	195	5.4	7.9	4.0	856	49	15	10
	1100	240	5.5	17	10	860	42	18	22
	1300	280	5.4	38	24	861	36	20.5	32
$In_{0.13}Ga_{0.87}As$ (type IV)	700	170	6.1	2.8	1.4	872	63	12	13
	900	180	5.0	6.2	3.1	875	50	15	16
	1100	200	4.5	18	9.5	876	48	16	28
	1300	240	4.6	34.5	19	879	44	17.5	34

Note: notations are the same as in Table 1.

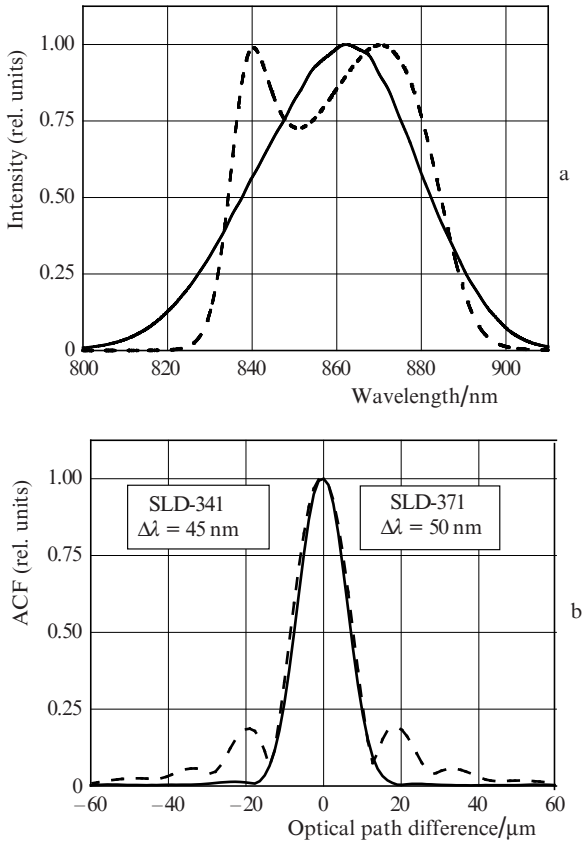

Figure 7. (a) Spectra of output radiation and (b) ACF central peaks of the commercial module SLD-371 (dashed curves) and the new module SLD-341 (solid curves).

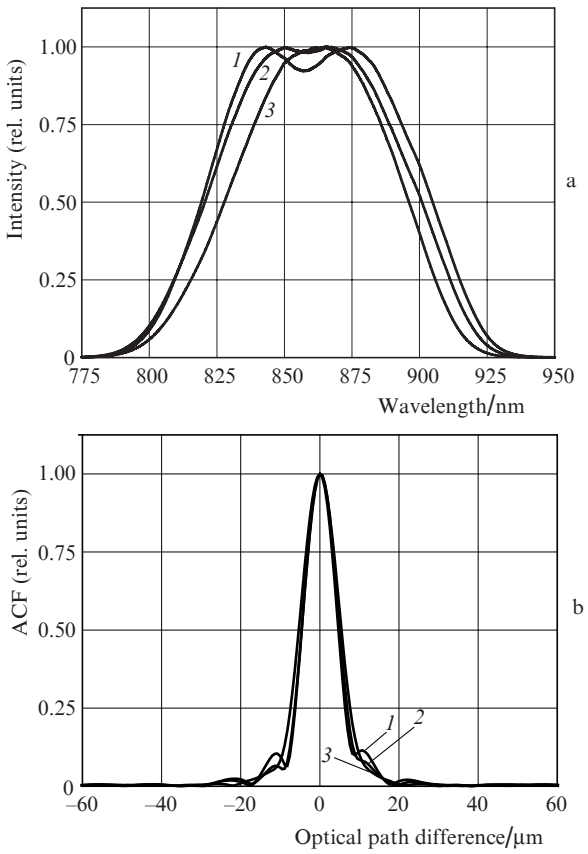

Figure 8. Superposition of type II and IV SLD emission spectra in different operation regimes (*1* – *3*) (a) and the corresponding ACF peaks (b).

4. Combined light sources with bell-shaped spectrum

Alongside with light-emitting SLD modules, in OCT systems and in optical metrology the combined light sources became widely used, in which the optical outputs of two or more broadband SLD modules with shifted spectra are joined by means of an optical coupler [5, 6]. An example is presented by the BroadLighter devices, produced in Russia. Their main advantages are high brightness and extremely low coherence. Unfortunately, the radiation spectrum of these sources has complex irregular shape and the height of the ACF pedestal amounts to 20%–25%.

As is known, a superposition of two shifted Gaussian-shaped spectra (1) with close FWHM under certain conditions allows obtaining a bell-shaped spectrum whose FWHM is close to the sum of FWHMs of the constituent spectra. The shape of such spectrum slightly differs from Gaussian, and the ACF pedestal is practically absent. This approach was used in the study of the prototypes of novel double-channel combined light sources on the basis of the developed SLD modules with the radiation output via a single-mode optical fibre. To join the output optical waveguides we used commercial fused couplers with the coupling ratios 50 : 50 or 40 : 60 for corresponding centre wavelengths. Figure 8 illustrates the output radiation spectrum shape optimisation process for one of the studied prototypes. In the present case the radiation was summed up from two modules on the base of SLDs of the types II and IV with $L_a = 1100$ μm. The shape of the resulting spectrum can be controlled within wide limits by varying the injection currents and operating temperatures of the SLDs, as well as by using single-mode fibre couplers with different dependences of the coupling ratio on the wavelength. In the considered case the aim was to obtain 'pure' ACF at maximal attainable spectral width and $P_{SM} > 5.0$ mW.

Table 3 summarises the basic technical characteristics of the implemented prototypes. The presented combinations of parameters with the bell-shaped spectrum are implemented

Table 3. Examples of basic characteristics of combined light sources with bell-shaped spectra based on the developed SLDs.

SLD types	L_a/μm	P_{SM}/mW	λ_m/nm	$\Delta\lambda$/nm	L_{coh}/μm
I + II	900	3.0	830	70	9.8
	1100	8.0	830	65	10.5
I + III	700	1.0	830	100	6.9
II+ IV	1100	7.0	860	80	9.2
	1300	20	860	70	10.5

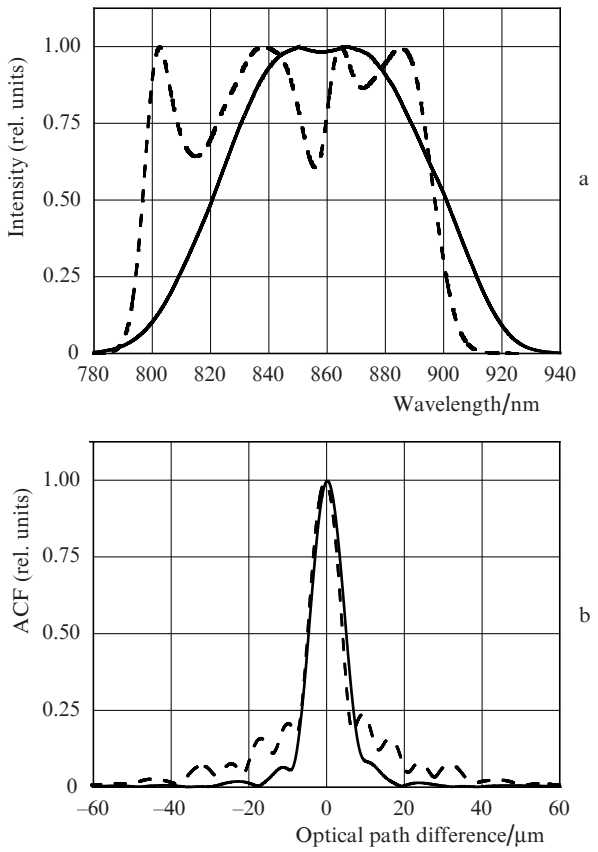

Figure 9. (a) Spectra of output radiation and (b) ACF central peaks of the commercial source model BroadLighter D-840-HP (dashed curves) and the new (preliminary D-860-G) model (solid curves).

for the first time. Among the commercially produced devices of the BroadLighter series, the model D-840-HP with the spectrum FWHM of nearly 100 nm is most popular. Figure 9 presents the emission spectra and ACF of this device and of the new model (preliminary designation D-860-G). There are all reasons to expect that for OCT systems the new device will be preferable.

5. Conclusions

The studies and development of SLD modules emitting in the 800–900 nm spectral range based on nanoheterostructures with the active layer thickness of a few nanometres are reported. The SLD modules possess a quasi-Gaussian spectrum shape with the width, exceeding by 2–3 times the spectral width of bulk SLDs in this spectral range. High reliability of the new devices is demonstrated. As a result of the performed studies, the commercial production of a new series of light-emitting modules having no analogues is started, namely, the SLD-34 series with the centre wavelengths 810, 840, 860, and 880 nm and continuous output power up to 50 mW into the free space and 25 mW via a single-mode optical fibre. The prototypes of the new broadband combined light sources with bell-shaped spectra are studied.

Acknowledgements. The authors express their gratitude to A.T. Semenov for initiating the present study, as well as to A.A. Zadernovskii for the discussion of the obtained results and valuable recommendations. The work was partially supported by the federal targeted programme The Scientists and Science Educators of Innovative Russia (Grant No. 14. B37.21.0756).

References

1. Drexler W., Fujimoto J.G. *Optical coherence tomography* (Berlin, Heidelberg: Springer-Verlag, 2008).
2. Batovrin V.K., Garmash I.A., Gelikonov V.M., Gelikonov G.V., Lyubarskii A.V., Plyavenek A.G., Safin S.A., Semenov A.T., Shidlovskii V.R., Shramenko M.V., Yakubovich A.D. *Kvantovaya Elektron.*, **23** (2), 113 (1996) [*Quantum Electron.*, **26** (2), 109 (1996)].
3. Kostin Yu., Lapin P., Shidlovski V., Yakubovich S. *Proc. SPIE Int. Soc. Opt. Eng.*, **7139**, 713905-1 (2008).
4. Il'chenko S.N., Ladugin M.A., Marmalyuk A.A., Yakubovich S.D. *Kvantovaya Elektron.*, **42** (11), 961 (2012) [*Quantum Electron.*, **42** (11), 961 (2012)].
5. Ko T.H., Adler D.C., Fujimoto J.G., Mamedov D.S., Prokhorov V.V., Shidlovski V.R., Yakubovich S.D. *Opt. Express*, **12** (10), 2112 (2004).
6. Adler D.S., Ko T.Kh., Konorev A.K., Mamedov D.S., Prokhorov V.V., Fujimoto J.J., Yakubovich S.D. *Kvantovaya Elektron.*, **34** (10), 915 (2004) [*Quantum Electron.*, **34** (10), 915 (2004)].